



**HAL**  
open science

## **Sustained calcium signalling and caspase-3 activation involve NMDA receptor in thymocytes in contact with dendritic cells**

Sylvia Cohen-Kaminsky, Pierre Affaticati, Olivier Mignen, Florence Jambou, Marie-Claude Potier, Isabelle Klingel-Schmitt, Jeril Degrouard, Roland Liblau, Thierry Capiod, Stéphane Peineau, et al.

### ► To cite this version:

Sylvia Cohen-Kaminsky, Pierre Affaticati, Olivier Mignen, Florence Jambou, Marie-Claude Potier, et al.. Sustained calcium signalling and caspase-3 activation involve NMDA receptor in thymocytes in contact with dendritic cells. *Cell Death and Differentiation*, 2010, 10.1038/cdd.2010.79 . hal-00550249

**HAL Id: hal-00550249**

**<https://hal.science/hal-00550249>**

Submitted on 25 Dec 2010

**HAL** is a multi-disciplinary open access archive for the deposit and dissemination of scientific research documents, whether they are published or not. The documents may come from teaching and research institutions in France or abroad, or from public or private research centers.

L'archive ouverte pluridisciplinaire **HAL**, est destinée au dépôt et à la diffusion de documents scientifiques de niveau recherche, publiés ou non, émanant des établissements d'enseignement et de recherche français ou étrangers, des laboratoires publics ou privés.

**Title:** Sustained calcium signalling and caspase-3 activation involve NMDA receptor in thymocytes in contact with dendritic cells

**Running title:** NMDAR calcium signalling in thymocytes

Pierre Affaticati<sup>1,2,3</sup>, Olivier Mignen<sup>2,1,3</sup>, Florence Jambou<sup>1,2,3</sup>, Marie-Claude Potier<sup>4</sup>, Isabelle Klingel-Schmitt<sup>1,2,3</sup>, Jeril Degrouard<sup>5</sup>, Stéphane Peineau<sup>6,7</sup>, Elodie Gouadon<sup>1,2,3</sup>, Graham L. Collingridge<sup>6</sup>, Roland Liblau<sup>8</sup>, Thierry Capiod<sup>9</sup> and Sylvia Cohen-Kaminsky<sup>1,2,3</sup>

<sup>1</sup>Centre National de la Recherche Scientifique (CNRS), Unité Mixte de Recherche UMR 8162, Institut Paris Sud Cytokines, Institut National de la Recherche Médicale, INSERM U999, Le Plessis Robinson, F-92350, France ;

<sup>2</sup>Université Paris-Sud, Orsay, F-91405, France ;

<sup>3</sup>Hôpital Marie Lannelongue, Le Plessis-Robinson, F-92350, France ;

<sup>4</sup>Centre National de la Recherche Scientifique (CNRS), Unité Mixte de Recherche UMR 7637, ESPCI, Paris, F-75005, France ;

<sup>5</sup>Centre National de la Recherche Scientifique (CNRS), Unité Mixte de Recherche UMR 8080, Département de Microscopie Electronique, Université Paris-Sud, Orsay, F-91405, France ;

<sup>6</sup>MRC Centre for Synaptic Plasticity, Department of Anatomy, School of Medical Sciences, Bristol, United Kingdom ;

<sup>7</sup> Institut National de la Recherche Médicale, INSERM, U676, Hôpital Robert Debré, Université Paris 7, Faculté de Médecine Denis Diderot Paris, F-75019, France ;

<sup>8</sup>Institut National de la Santé et de la Recherche Médicale, INSERM U563, Hôpital Universitaire Purpan, Toulouse, F-31000, France ;

<sup>9</sup>Institut National de la Santé et de la Recherche Médicale, INSERM, U1003, IFR147, Université Lille 1, Villeneuve d'Ascq, F-59655, France.

**Corresponding author:** Sylvia Cohen-Kaminsky, INSERM U999, Université Paris Sud, Hôpital Marie Lannelongue, 133 Avenue de la Résistance, F-92350, Le Plessis-Robinson, France

E-mail: [sylvia.cohen-kaminsky@u-psud.fr](mailto:sylvia.cohen-kaminsky@u-psud.fr) Phone: 33 1 40 94 25 14 Fax: 33 1 40 94 25 22

## ABSTRACT

L-glutamate, the major excitatory neurotransmitter, also plays a role in non-neuronal tissues and modulates immune responses. Whether NMDA receptor (NMDAR) signalling is involved in T cell development is unknown. Here we show that mouse thymocytes expressed an array of glutamate receptors, including NMDARs subunits. Sustained calcium signals, and caspase-3 activation in thymocytes were induced by interaction with antigen-pulsed DCs and were inhibited by NMDAR antagonists MK801 and memantine. NMDAR was transiently activated, triggered the sustained calcium signal, and was corecruited with the PDZ-domain adaptor PSD-95 to thymocyte-DC contact zones. While T cell receptor (TCR) activation was sufficient for relocalization of NMDAR and PSD-95 at the contact zone, NMDAR could be activated only in a synaptic context. In these T-DC contacts, thymocyte activation occurred in the absence of exogenous glutamate, indicating that DCs could be a physiological source of glutamate. DCs expressed glutamate, glutamate-specific vesicular VGLUT transporters and were capable of fast glutamate release through a  $Ca^{2+}$ -dependent mechanism. We propose that glutamate released by DCs could elicit focal responses through NMDAR-signalling in T cells undergoing apoptosis. Thus, synapses between T and DCs could provide a functional platform for coupling TCR activation and NMDAR signalling which might reflect on T cell development and modulation of the immune response.

**Key words:** Calcium signalling / thymocyte / NMDAR

**Abbreviations:** APC, antigen-presenting cell;  $\text{Ca}^{2+}$ , calcium; CRAC,  $\text{Ca}^{2+}$  release-activated  $\text{Ca}^{2+}$ ; DC, dendritic cell; DP,  $\text{CD4}^+\text{CD8}^+$  double-positive, GluR, glutamate receptor; iGluR, ionotropic glutamate receptor; IS, immunological synapse; mGluR, metabotropic glutamate receptor; NMDA, N-methyl-D-aspartate, NMDAR, NMDA receptor; PSD, post-synaptic density; siRNA, small interfering RNA; TCR, T cell receptor; VGLUT, vesicular glutamate transporter.

## INTRODUCTION

L-glutamate is the major excitatory neurotransmitter in the nervous system. The N-methyl-D-aspartate (NMDA) receptor belongs to the ionotropic glutamate receptors (iGluRs), mediates fast synaptic responses<sup>1</sup>, and is involved in neuronal synaptic transmission and plasticity by fine-tuning  $\text{Ca}^{2+}$  signalling<sup>2</sup>. There is now evidence to suggest that glutamate acts as a signalling molecule in non-neuronal tissues<sup>3,4</sup>, with an emerging role as an immune modulator<sup>5</sup>. Metabotropic G-protein-coupled GluRs (mGluRs) are involved in T-cell activation<sup>6</sup>, and in the inhibition of activation-induced cell death<sup>7</sup>. iGluRs are involved in cell cycle progression, regulating activation and proliferation, chemotactic migration and integrin-mediated adhesion in T cells<sup>8-10</sup>, with some indications for a role of the NMDAR in  $\text{Ca}^{2+}$  signalling<sup>11,12</sup>.

Increases in  $[\text{Ca}^{2+}]_i$  are key signals in T-cell activation following TCR engagement. T lymphocytes are believed to use store operated calcium (SOC) channel entry as the main mode of calcium influx<sup>13</sup>. The SOC channels in lymphocytes are known as CRAC channels, whose molecular identity has been recently elucidated, with Orai1 as the pore forming subunit and STIM1 as the sensor of stored calcium<sup>14</sup>. Orai1 and STIM1 are recruited to the immunological synapse<sup>15</sup>. Although CRAC plays a major role in T cells<sup>13</sup>, it is likely that their complex  $\text{Ca}^{2+}$  signalling also involves purinergic receptors, voltage-gated  $\text{Ca}^{2+}$  channels, and modulation by  $\text{Ca}^{2+}$ -dependent voltage-activated  $\text{K}^+$

channels<sup>14,16</sup>. Elucidating the relationships between all these routes of cytosolic calcium modulation remains a challenge for the future. Until recently, most of the studies exploring Ca<sup>2+</sup> entries in T cells, especially glutamate receptor entry, were not carried out under physiological stimulation by antigen-presenting cells.

The immunological synapse (IS) is a structure which mediates information exchange that typically forms in the contact zone between an antigen-presenting cell (APC) and a T cell bearing a specific TCR. It was first suggested to facilitate the directed secretion of cytokines between T cells and APCs<sup>17</sup>. Cytokines may be released directly into the synapse, having an immediate effect on clustered receptors in the contact zone<sup>18</sup>. The synapse formed between T cells and dendritic cells (DCs) displays cell-to-cell adhesion, stability and close apposition of membranes<sup>19</sup>, that may help to optimize soluble mediator concentration at the T cell-APC interface, thereby limiting effects on bystander cells. Neuronal synapses and ISs are often compared due to their anatomical similarity, although ISs form rapidly and are transient<sup>20</sup>. To what extent these synapses are functionally similar is not known.

Circulating T cells are thought to be exposed to glutamate in the plasma, glutamate-rich peripheral organs<sup>3,4</sup>, and in the brain, facilitating crosstalk with the nervous system<sup>21</sup>. It is therefore likely that GluRs are not permanently stimulated in T cells, and we postulated that their activation occurs as a result of IS formation. In analogy to neurons, glutamate should therefore be rapidly released, with faster kinetics than those reported through the cystine/glutamate antiporter (X<sub>c</sub><sup>-</sup> system)<sup>22</sup>. Indeed, the possibility that glutamate released by APCs at ISs mediates communication with T cells through GluR-mediated Ca<sup>2+</sup> signalling has never been investigated.

Since glutamate mediates apoptosis of neuronal cells through NMDARs and Ca<sup>2+</sup> signalling<sup>23</sup>, we investigated thymocyte development, a fundamental process in which developing T cells that recognize self-antigens with high affinity are eliminated by Ca<sup>2+</sup>-dependent apoptosis following

their close interaction with DCs<sup>24</sup>. Our findings indicate that DCs are capable of fast calcium-dependent glutamate release, while thymocytes express NMDARs, which modulate TCR-dependent Ca<sup>2+</sup> signalling and apoptosis only in a synaptic context, revealing a novel aspect of IS functioning.

## RESULTS

### NMDARs are expressed in thymocytes

More than 30 different GluRs are expressed in the central nervous system (CNS)<sup>1</sup>. Since only mGluRs have been detected in thymocytes<sup>25</sup>, we used neurotransmission-dedicated oligoarrays to analyze their GluR repertoire. Thymocytes expressed most known GluRs (Supplementary Figure S1a), including NMDAR GluN1, GluN2A and GluN2B subunits (IUPHAR nomenclature of subunits, previously referred to as NR1, NR2A and NR2B subunits<sup>26</sup> (Figure 1a). These findings were confirmed by PCR (Figure 1a), and confocal microscopy, using well-characterized antibodies (Figure 1b, Supplementary Figure S1c). To study NMDAR function, we focused on GluN1, the obligate subunit of NMDARs which was expressed in thymocytes at a level similar to what was observed in the brain (Figure 1a, Supplementary table S1). FACS analysis, using antibodies that detect NR1 as a band at the expected molecular weight by Western blotting in brain microsomal preparations, indicated that 97.3% of thymocytes expressed NR1, with higher expression in CD4<sup>+</sup> or CD8<sup>+</sup> cells as compared to DP cells (Figure 1c).

### Calcium signalling and apoptosis in thymocytes in contact with DCs, involves NMDAR

To explore NMDAR function in thymocytes, we focused on Ca<sup>2+</sup> and apoptosis signalling. Indeed, both are associated with NMDAR activity in neurones. Glutamate and NMDA, at doses of 1 to 500  $\mu$ M, did not induce Ca<sup>2+</sup> signalling nor apoptosis in freshly isolated thymocytes (data not shown).

Thus, we investigated whether a thymocyte-DC synaptic context could provide the environment required for coupling  $\text{Ca}^{2+}$  signalling to apoptosis.

To set-up an *in vitro* system of T cell-DC contacts, we used HNT-TCR-transgenic mice in which most T cells express the same TCR directed to the HA126-138 peptide. *In vivo* administration of the antigenic HA126-138 peptide in HNT-TCR transgenic mice was shown to induce massive apoptosis, mostly of  $\text{CD4}^+\text{CD8}^+$  double-positive (DP) thymocytes <sup>27</sup>. Thus we cocultured thymocytes from HNT-TCR-transgenic mice and HA-peptide pulsed DCs, to enhance the probability to observe antigen-dependent synaptic contacts between thymocytes and DCs. To assess the presence of functional synaptic contacts, we monitored DC capacity to induce thymocyte apoptosis by following the expression of three markers. The first one, Nur77 is an immediate early gene required for the induction of apoptosis in negative selection <sup>28</sup>, and a specific marker of clonal deletion *in vivo* <sup>29</sup>. The second, CD69 is an early T-cell activation marker up-regulated after TCR engagement, and involved in negative selection <sup>30</sup> and was thus used to discriminate thymocytes that have formed synapses with DCs. To analyze apoptosis we used activated caspase-3 in living cells, allowing early detection of apoptosis and avoiding by-stander effects occurring at later time points. These three markers of thymocyte activation and clonal deletion expressed during negative selection *in vivo* (Nur77, CD69, and activated caspase-3), that we measured in our own *in vivo* experiments, were also upregulated in our *in vitro* model, assessing the presence of functional synapses (Supplementary Figure S2a). In contrast to thymocytes, peripheral  $\text{CD4}^+$  T cells in contact with DCs showed increased CD69 expression, without caspase-3 activation (Supplementary Figure S2b) and proliferated as expected in response to HA peptide (data not shown).

Then we used this *in vitro* system to monitor the calcium signal elicited in single thymocytes by contact with antigen-pulsed DCs, in the absence of exogenous glutamate. Antigen-specific contacts of thymocytes with DCs, in a glutamate-free medium, resulted in rapid and sustained increases in

$[Ca^{2+}]_i$  in T cells (Figure 2a and b). Most thymocytes established long-lasting contacts, 90 % of which resulted in a  $Ca^{2+}$  peak ( $\Delta R/R=2.93\pm 0.08$ ,  $n=119$ ), followed by a sustained high-level plateau lasting at least 10 minutes (Figure 2b and Supplementary Video S1). A few unstable contacts with no measurable  $Ca^{2+}$  signals were observed in the absence of HA-peptide (Figure 2b). Interestingly, contacts with purified peripheral splenic  $CD4^+$  T cells resulted in a  $Ca^{2+}$  signal with a peak similar to that for thymocytes ( $\Delta R/R=3.72\pm 0.19$ ,  $n=32$ ), but rapidly decreasing (50 % decrease from the peak value in  $91\pm 13$  s,  $n=30$ ) to a plateau maintained at a basal level of about one fifth of the peak value (Figure 2a and c, Supplementary Videos S1 and S2).

Thus, thymocyte-DC contact in the absence of exogenous glutamate results in sustained calcium signalling with a high plateau and apoptosis signalling. These results also point to a potential relationship between the sustained shape of the  $Ca^{2+}$  signal and T cell fate.

### **NMDAR triggers the sustained calcium response in thymocytes and is involved in thymocyte apoptosis**

The primary mechanism of  $Ca^{2+}$  mobilization in T cells is the release of  $Ca^{2+}$  from intracellular stores followed by  $Ca^{2+}$  influx through  $Ca^{2+}$  release-activated  $Ca^{2+}$  (CRAC) channels<sup>13</sup>. We hypothesized that NMDARs might participate in  $Ca^{2+}$  influx, thereby contributing to the sustained  $Ca^{2+}$  plateau observed during thymocyte apoptosis.

As previously mentioned, exogenous glutamate or NMDA did not induce any  $Ca^{2+}$  signalling in freshly dissociated thymocytes. Patch-Clamp recordings of these thymocytes confirmed that no NMDA current was detectable, when exogenous NMDA and D-serine were co-applied before any synaptic contact with DC (data not shown). In the T cell-DC contact model, we incubated T cells either with MK801 or memantine, two non-competitive open-channel NMDAR blockers, and then measured T cell-DC contact-induced  $Ca^{2+}$  signals and apoptosis in presence of these inhibitors.



MK801 and memantine modulated  $\text{Ca}^{2+}$  signals in about 50% of thymocytes, resulting in a transient signal with a similar amplitude at the initial peak ( $3.15 \pm 0.14$ ,  $n=42$  and  $2.81 \pm 0.12$ ,  $n=33$ , for MK801 and memantine respectively) to control cells, but with a plateau close to basal levels (50% decrease in the peak value after  $148 \pm 16$  s,  $n=18$  and  $275 \pm 37$  s,  $n=14$ , respectively) (Figure 2d and Supplementary Video S3).

These blockers also significantly affected the percentages of activated caspase-3-expressing cells ( $27 \pm 0.7\%$  inhibition with MK801,  $n=24$  and  $30 \pm 0.85\%$  with memantine,  $n=15$ ) (Figure 3a), indicating a role for NMDARs in apoptosis. Of note, the effect on caspase-3 expression might be underestimated since only 50% of the thymocytes engaged in a synapse were sensitive to the drugs, as measured in  $\text{Ca}^{2+}$  signalling experiments, as mentioned above. Activation of Nur77 expression, which is  $\text{Ca}^{2+}$ -dependent<sup>31</sup>, was affected by MK801 as measured by FACS analysis 4 hours after thymocyte-DC contact (Figure 3b and c), suggesting that Nur77 could be an early target of the  $\text{Ca}^{2+}$  signal mediated by NMDAR. To rule out the possibility that NMDAR blockers had non-specific effects on CRAC or other off-target effects on channels involved in T-cell activation, we monitored the  $\text{Ca}^{2+}$  signal by FACS on a large thymocyte population, activated by biotinylated anti-CD3 and anti-CD28 antibodies followed by streptavidin cross-linking, in the absence of glutamate. About 60% of thymocytes responded to TCR stimulation by a  $\text{Ca}^{2+}$  signal that was unaffected by MK801 or memantine (Supplementary Figure S3), indicating that these drugs had no major effect on  $\text{Ca}^{2+}$  signalling resulting from TCR triggering.

These results (NMDA insensitivity of freshly isolated thymocytes and MK801/memantine inhibition of  $\text{Ca}^{2+}$  and apoptosis signalling in DC contacting thymocytes) suggest that NMDA channels are activated only during or after synapse formation. To further investigate the involvement of NMDA channels in this process, we ask if 1) NMDARs are activated only after synapse formation and 2) the sustained  $\text{Ca}^{2+}$  response required a transient NMDAR activation. Using the T cell-DC contact model,

we firstly incubated freshly dissociated T cells with MK801, NMDA and D-serine. In these conditions MK801 will definitely block all activable NMDARs present at the membrane. We then washed the thymocytes and, in presence of DCs, recorded the  $Ca^{2+}$  signalling following synaptic contact. The sustained  $Ca^{2+}$  responses recorded (n=47, 95% of cells with a sustained signal) (Figure 3d), were similar to the responses recorded in absence of T cell pre-treatment, suggesting that NMDARs are active only after synaptic contact even if their agonists are present. In the same conditions of pre-treatment of thymocytes with MK801, NMDA and D-serine, addition of MK801 in the bath solution before synapse formation, revealed a sensitivity of the  $Ca^{2+}$  plateau to this NMDAR blocker (n=22, 55% of cells with a transient signal) (Figure 3d). Using the same protocol, 200 seconds after the beginning of  $Ca^{2+}$  signalling due to T cell-DC contacts, we applied MK801. MK801 application after synapse formation failed to inhibit  $Ca^{2+}$  response (n=20, 90% of cells with a sustained signal) (Figure 3e). Together these results suggest that NMDARs are necessary for the induction of the sustained  $Ca^{2+}$  response but are only transiently activated at the beginning of the synaptic response. Furthermore these receptors are also involved in the induction of the thymocyte apoptosis after contact with DCs

### **Thymocyte-DC interaction induces GluN1 and PSD-95 clustering at the contact zone.**

Transient activation of NMDA channels at the synapse suggest that an important trafficking of these receptors could occur in thymocytes. The TCR signalosome includes PDZ domain-containing adaptors, initially described at neuronal synapses but increasingly thought to be involved in ISs<sup>32</sup>. PSD-95, a prototypical PDZ domain protein, accumulates in the active zones of neuronal synapses, forming so-called postsynaptic densities (PSDs). It is the first-line signalling adaptor binding directly to the C-terminus of NMDAR subunits<sup>33</sup>, involved in stabilization and functional recruitment of NMDARs at the excitatory synapse<sup>34</sup>. Staining for GluN1 and PSD-95 indicated that both were distributed over the entire resting thymocytes, but were colocalized in the contact zone in

T cell-DC synapses (Figure 4a, and Supplementary Figure S4). When T cells were stimulated with anti-CD3/CD28-coated beads in the absence of glutamate, PSD-95 was nonetheless colocalized with GluN1 in the contact zone (Figure 4a) indicating that the relocation of NMDAR and PSD-95 to the synapse depends on TCR stimulation. Interestingly, TCR stimulation using anti-CD3/CD28 coated beads, in the presence or absence of NMDA (or glutamate itself), did not recapitulate the effect of glutamate observed in a synaptic context. The  $\text{Ca}^{2+}$  signal was not sustained with a high level plateau (Figure 4b and c), no significant apoptosis was induced (data not shown) and no NMDA current were recorded (data not shown), indicating that in addition to glutamate, one or several other signals provided by the DC, are necessary to activate NMDARs.

We conclude that intense trafficking of NMDAR may occur in thymocytes upon contact with DCs. The TCR triggering is sufficient to induce GluN1 and PSD-95 clustering at the synapse, while the NMDAR is activated only in a complete synaptic context.

### **DCs are capable of fast glutamate release**

Since all the  $\text{Ca}^{2+}$  signalling experiments in T cells contacting DCs were performed in the absence of exogenous glutamate, we wondered which cell was the physiological source of glutamate in T cell-DC synapses. Immunostaining and confocal microscopy with a specific antibody to glutamate indicated that DCs were probably the principal source of glutamate in T cell-DC synapses (Figure 5a). Moreover, DCs express the glutamate-specific vesicular transporters VGLUT1 and VGLUT2, which confer a glutamatergic phenotype to neurons<sup>35</sup> and VGLUT3 (Figure 5b and Supplementary Figure S5b). Vesicular structures of 100 nm size, with a characteristic electron-dense membrane were observed in DCs, opposite the contact zone and often located in a polarized cytoplasmic region containing mitochondria (Figure 5c). Immunogold labeling of VGLUT2 showed clusters of particles delineating discrete vesicles, opposite the contact zone in DCs (Figure 5d and Supplementary Figure

S5d). Purified DCs express mRNAs encoding components involved in neurotransmitter exocytosis via SNARE complex formation (synaptophysin, Snap-23, VAMP-2) or in the regulation of vesicle docking (Munc-18), as well as synaptotagmin-I (Supplementary Figure S5c and e), a  $\text{Ca}^{2+}$  sensor for glutamate release<sup>36</sup>. Double immunogold labelling showed that VGLUT2 and synaptotagmin-I were expressed in the same vesicular structures (Figure 5e), suggesting the presence in DCs of a compartment competent for both glutamate accumulation and exocytosis. The question of glutamate production by immune cells was previously addressed, by measuring glutamate accumulation starting from 24 hours in supernatants of monocyte-derived DCs and in T-DC cocultures<sup>22</sup>. Instead, we focused on direct monitoring of glutamate release, in real time, by freshly isolated DCs. We used the L-glutamate dehydrogenase-linked assay, a fluorescence-based assay allowing dynamic quantification of glutamate release in non-excitabile cells, to monitor in real time rapid glutamate release from DCs<sup>37</sup>. In the presence of external  $\text{Ca}^{2+}$ , ionomycin (Figure 5f) and SDF-1 $\alpha$  (a physiological stimulus identified for astrocytes<sup>38,39</sup> (Figure 5g) triggered both  $[\text{Ca}^{2+}]_i$  increases and glutamate release in DCs with a similar time course.

We conclude that DCs exhibit features required for regulated glutamate exocytosis and are capable of fast glutamate release in a  $\text{Ca}^{2+}$ -dependent manner.

## DISCUSSION

In previous studies, GluRs were potentially involved in immune regulation<sup>5</sup>, T cells were thought to be exposed to glutamate in the CNS, in the bloodstream or in certain peripheral organs<sup>9</sup> and monocyte derived DCs have been pointed out as a source of slow glutamate release accumulating in T-DC long term-cocultures<sup>22</sup>. As T cells communicate through ISs, which are structurally similar to neuronal synapses<sup>20</sup>, several questions are left unanswered. Does the IS use glutamate signalling? Is

that signalling linked to  $\text{Ca}^{2+}$  signals governing T-cell fate? How important is synapse structure in glutamatergic communication between T cells and DCs? To what extent are immunological and neuronal synapses functionally similar?

### **The NMDAR, a $\text{Ca}^{2+}$ entry in T cell signalling at the IS**

Until recently, most of the studies exploring  $\text{Ca}^{2+}$  entries in T cells were not carried out on T cells contacting APCs. We observed NR1 expression in the majority of resting thymocytes, which responded to DC contact with an immediate calcium signal, with a sustained plateau sensitive to NMDAR blockers. Our data suggest that this sustained  $\text{Ca}^{2+}$  signal that occurs in thymocytes contacting DCs is probably not due to a sustained activity of the NMDAR. Similarly to the mechanism involved in synaptic plasticity (Long Term Depression (LTD) and Long Term Potentiation (LTP)) of nervous synapses<sup>40</sup> there might be a transient activation of the NMDAR, which could act as a trigger of a sustained  $\text{Ca}^{2+}$  response carried by other effectors. However, no detectable NMDAR signal was observed in resting thymocytes and in thymocytes stimulated with anti-CD3/CD28 coated beads (ie not engaged in a full synapse with DCs). It is physiologically relevant that the contact with DC may be necessary to activate NMDARs. Our observation that sustained  $\text{Ca}^{2+}$  signalling and apoptosis occurred only in the context of IS and not in solitary thymocytes is in line with the need for a tight control of T-cell activation by antigen-specific contact with DC, to ensure proper thymic negative selection. Indeed, the IS is the physiological structure dedicated to communication in the immune system and represents a logical strategy to provide protection against permanent exposure of thymocytes to glutamate. Such a strategy could also make sense in activation of peripheral T cells which are exposed to serum glutamate concentrations. The sustained, high-level  $\text{Ca}^{2+}$  plateau observed in this study was characteristic of thymocytes and correlated with antigen-dependent induction of apoptosis. It was not observed in naïve peripheral  $\text{CD4}^+$  splenic T cells that displayed glutamate

signalling-dependent proliferation (P.A. and S.C-K unpublished data) but no apoptosis (Supplementary Figure S2b). The correlation between T-cell fate and the shape of the  $\text{Ca}^{2+}$  signal suggests that the elevated plateau phase is intimately linked to thymocyte apoptosis. This opens new challenges to identify the switches controlling pro-survival vs pro-apoptosis outcome of NMDAR stimulation.

### **Dendritic cells, a site of glutamate mobilization for exocytosis**

A recent study of T cells in coculture with monocyte-derived DCs pulsed with a superantigen, showed glutamate production in the milieu, detectable from day 1 (in the 5  $\mu\text{M}$  range) and accumulating in the coculture supernatant with time. This glutamate production involved a slow release mechanism, mediated by the cystine/glutamate antiporter  $\text{X}_c^-$  system, and glutamate was suggested to activate mGluRs in T cells<sup>22</sup>. Here, we demonstrated in real time a rapid and substantial release of glutamate by DCs, consistent with previous reports of synaptic polarization and  $\text{Ca}^{2+}$ -regulated release of pre-assembled vesicular cytokine stores for DCs<sup>41</sup>. We used several approaches to suggest that DCs are competent for both glutamate accumulation and release. 1) Immunofluorescence studies showed specific, strong punctate staining for glutamate and VGLUT vesicular transporters, and staining for the calcium sensor synaptotagmin-I and VAMP-2, a SNARE component of the vesicular machinery for exocytosis. 2) Electron microscopy showed that vesicle-like structures were present in the T cell-DC contact zones. 3) Electron microscopy and double staining with gold particles suggested that DCs are competent for both the glutamate accumulation mediated by VGLUT vesicular transporters and for glutamate release through a calcium- and SNARE-dependent mechanism. 4) Finally, an enzymatic-linked assay demonstrated ionomycin and SDF-1 $\alpha$ -induced L-glutamate release by DCs. Experimental studies of the mechanism of glutamate release were beyond the scope of this study. It remains to define the precise SNARE-dependent

mechanism of exocytosis, using specific drugs or toxins, and to determine the type of  $\text{Ca}^{2+}$  entry involved in exocytosis signalling; mechanisms similar to those reported for astrocytes might be expected<sup>38</sup>. In our hands, riluzole and bafilomycin inhibited the calcium signal and caspase-3 induction in thymocytes contacting DCs (P.A and SC-K unpublished data). However, this approach is not entirely appropriate as these drugs as well as specific toxins would target the exocytosis of compounds other than glutamate, such as chemokines. Indeed, as in astrocytes<sup>38</sup> we have shown that SDF-1 $\alpha$ , a physiological stimulus mobilizing intracellular  $\text{Ca}^{2+}$ , triggers the release of glutamate from DCs. How SDF-1 operates in the minimal system of T-DC synapses for glutamate release remains to be determined. In addition, it is difficult to demonstrate glutamate release in the synaptic cleft directly because of the dynamic nature of the synapse (Supplementary videos S1-S3).  $\text{Ca}^{2+}$  transients in DCs interacting with T cells may be involved in triggering glutamate exocytosis, but they have rarely been observed in our study (data not shown), rather suggesting that local  $\text{Ca}^{2+}$  fluxes in DCs might be involved in glutamate release. Since thymic epithelial cells, did not release measurable glutamate in real-time (P.A., T.C. and S.C-K, unpublished data), DCs may be specialized for rapid glutamate delivery to T cells. Glutamate should be considered an “immunotransmitter” as suggested for cytokines and chemokines<sup>42</sup>.

### **PSD-95, a signalling adaptor indicative of the glutamatergic phenotype of the IS**

In neuronal synapses, PSDs, which contain an intricate network of scaffolding PDZ-domain proteins, are thought to participate in synapse genesis and to organize  $\text{Ca}^{2+}$  sources, sensors and effectors, and a number of signalling proteins<sup>43</sup>. Several studies have described a role for PDZ-domain proteins, e.g. CARMA1 and hDlg/Dlg1/SAP97 have been implicated in T-cell activation<sup>44</sup>, and TCR activation-induced synapse assembly<sup>32</sup>, respectively. Our findings add to the current knowledge the possibility of PSD-95-mediated connections between NMDARs and TCRs. While

the role of GluRs in communication between thymocytes and DCs was not entirely unexpected, we were surprised to find that an event associated with TCR triggering alone was sufficient to promote the clustering of both NMDAR and PSD-95 in the contact zone. We suggest that TCR signalling triggers the modeling of the nascent IS into a functionally competent synapse for glutamate signalling. Hence, our data indicated that NMDAR can be activated only in the context of a synapse (Figure 4a). An additional signal from the DC may be needed to activate NMDARs and/or the timing of exposure to glutamate relative to TCR activation may be critical to activate NMDARs. Thus, we propose that the IS may provide a functional platform for coupling detection of TCR ligation and GluR activation with subsequent focal GluR signalling. PSD-95 may well be a primary adaptor, connecting TCR and NMDAR signalling. A challenge will be to understand the precise molecular mechanism of the interconnection between TCR and NMDAR signalling. Furthermore, a transient activation of NMDARs at the synapse would suggest that an important trafficking of these receptors could occur in thymocytes. Although our data indicate that PSD95 might be involved, the mechanism of NMDAR exocytosis at the synapse as demonstrated in neurones<sup>40</sup> remains to be solved.

### **Conclusions and clinical consequences**

For years, glutamate signalling was thought to take place primarily in the CNS; it is now known to control key peripheral physiological functions, such as insulin secretion, keratinocyte differentiation, and remodeling of bone mass. Accordingly, therapeutic applications are being developed for diabetes, psoriasis, and osteoporosis<sup>4</sup>. Our findings provide insights into an additional site of peripheral glutamate signalling and possible involvement of NMDARs in a major physiological function of the thymus, the negative selection of unwanted and potentially harmful developing T cells, preventing their export to the periphery<sup>45</sup>. There is still a long road to solve the complexity of the cooperation of different GluRs in T-DC synapses, as defined in neuronal synapses.



Understanding the precise role of glutamate signalling in a diversity of immune responses and in determining T-cell fate by modulating the proliferation/differentiation balance, the effector/regulatory and effector/memory transitions, might reflect on the physiology of the adaptive immune response.

Our findings together with previous data<sup>5</sup> raise potential applications for drug-mediated immunomodulation through interactions with L-glutamate signalling. Drugs targeting peripheral GluRs without affecting the CNS are under development. Conversely, the impact on immune competence of drugs used in the CNS should also be examined carefully. The idea that neurodegenerative diseases involving defects in glutamatergic transmission are often associated with immune dysregulation is emerging, but has not yet been fully explored. It would be very interesting to evaluate precisely the immune status of patients with such diseases.

## **MATERIAL AND METHODS**

### **Mice**

The generation and genotyping of HNT-TCR transgenic mice specific for the HA 126-138 (HNTNGVTAACSHE) peptide presented by MHCclass II I-A<sup>d</sup> have been described elsewhere<sup>27</sup>. All animals had a B10.D2 (H2<sup>d</sup>) genetic background and were used at the age of 6 to 10 weeks. All animal experiments conformed to European Community guidelines of animal protection and local legal and ethical requirements. All experiments were approved by local authorities and direction des Services Veterinaires des Hauts-De-Seine (authorization for animal experimentation to SC-K, N°92-131). T cells and DCs were isolated, purified and cocultured using standard methods as described in Supplemental online Material and Methods.

### **Antibodies and reagents**

All antibodies were proved to be specific and are widely used in the neuronal system. Antibodies against NR2A and NR2B were purchased from Upstate Biotechnology. Antibodies against NR1 (M68), VGLUT1, VGLUT2 and VGLUT3 used in flow cytometry or confocal microscopy were from Synaptic Systems. Anti-NR1 antibody M68, widely used in neurones, recognized a band at the expected molecular weight (116KD) in western blotting experiments of thymocytes extracts immunoprecipitated by anti-PSD-95 (data not shown). Biotinylated anti-CD3 (145-2C11) and anti-CD28 (37.51) were from Pharmingen. Antibodies against PSD-95 and glutamate were from Zymed and Sigma, respectively. All inhibitors and antagonists specific for GluRs were from Tocris.

### **DNA Chip analysis of the GluR repertoire**

DNA chip analysis was performed on Neurotrans NT280M oligochips from GeneScore ([www.genescore.fr](http://www.genescore.fr)), registered on GEO (Gene Expression Omnibus) (N° GPL4746), already used for studies in the CNS and containing oligonucleotides for 280 genes involved in neurotransmission (2 oligonucleotides for each gene).<sup>46</sup> Modifications are available in Supplemental online Material and Methods.

**Single-cell Ca<sup>2+</sup> video imaging** Single-cell Ca<sup>2+</sup> video imaging on T cell-DC conjugates was carried out using a modified version of a previously described method.<sup>47</sup> Purified DCs were plated on glass delta T culture dishes (Biopetechs) coated with polylysine and maintained at 37°C in recording solution (mammalian saline: 116 mM NaCl, 5.6 mM KCl, 1.2 mM MgCl<sub>2</sub>, 2 mM CaCl<sub>2</sub>, 5 mM NaHCO<sub>3</sub>, 1 mM NaH<sub>2</sub>PO<sub>4</sub>, 20 mM HEPES, pH 7.3, supplemented with 2 g/l glucose). Thymocytes or CD4<sup>+</sup> T cells were loaded for 30 minutes with 4 μM Fura-2/AM (Molecular Probes) by incubation for 30 minutes at 37°C in culture medium. When indicated T cells were preincubated for

10 minutes with the NMDAR antagonists and then dispensed on top of the DCs maintained at 37°C using a temperature-controlled dish, that was fixed above a warmed epifluorescence 40 x oil objective (Bioptechs) and a PTR 200 perfusion temperature regulator (ALA Scientific Instruments, Westbury, NY, USA). Successive fluorescence and DIC images were recorded for 20 minutes. Light for excitation was supplied by a high pressure 100 W xenon arc lamp and the 340 and 380 nm wavelengths were selected with a monochromator (Cairn Research Ltd). Fluorescence images were collected with a Sensicam QE CCD camera (PCO Computer Optics GmbH), digitized, and integrated in real time by an image processor (Metafluor©). The light transmission images were taken every 6 s, alternating with the fluorescent images. The fluorescent signals were analyzed offline, using an image processor (Metamorph©) to account for cell movements during the 20-minute recordings. Background fluorescence was subtracted from the corresponding fluorescent images. To allow comparison between different labs, results are expressed as  $(\Delta R/R)$ , where R is the ratio (R) between fluorescence signals at 340 and 380 nm obtained before the addition of any agent, and  $\Delta R$  the difference between the ratios measured during a response and R. For single cell  $Ca^{2+}$  video imaging in isolated thymocytes and DCs, a modification of this protocol was used and is provided in Supplemental online Material and Methods.

### **Extracellular glutamate imaging**

We monitored glutamate efflux in continuous culture, using a well characterized enzymatic assay.<sup>37</sup> Purified DCs ( $5 \times 10^5$ ) were incubated for 20 minutes on glass coverslips treated with polylysine, to allow adhesion. DCs were washed and bathed in the recording solution (mammalian saline as above, supplemented with NAD (1mM), and L-glutamate dehydrogenase (GDH) at 50 IU/ml (Sigma). Glutamate released from the cells was immediately oxidized to  $\alpha$ -ketoglutarate by GDH, with the formation of NADH and fluorescence emission at 450 nm. Controls without L-GDH indicated that

detectable levels of NADH are not produced by DCs, either spontaneously or after induction by ionomycin. Agents were added directly to the culture dish.

### **Flow cytometry and confocal microscopy**

Flow cytometry (four color flow cytometry, activated caspase-3 detection and calcium flux studies) and confocal microscopy on T cell-DC conjugates were performed using standard procedures as described in Supplemental online material. The controls consisted of mouse isotype controls (as control for the monoclonal M68 anti-NR1, anti-Nur77 and anti-synaptotagmine antibodies), and purified rabbit IgG as control for anti-NR2A, NR2B, GluR2/3, PSD-95, KA2, glutamate, VGLUT antibodies. The same settings and exposure time were used for image acquisition by confocal microscopy of the specific staining and the controls.

### **Electron microscopy**

Morphological analysis and post-embedding immunocytochemistry and immunogold labelling of T cell-DC conjugates was performed using classical techniques as described in Supplemental online Material and Methods. Mouse isotype controls and purified rabbit IgG were used as controls for immunogold staining, with the same exposure time and magnification as specific staining.

### **Statistical analysis**

Data are expressed as means  $\pm$  SEM. Statistical significance was assessed by the non-parametric Mann-Whitney test, using Prism, version 5.0, software (GraphPad Software, San Diego, CA). The significance level was set at P equals .05. The Kolmogorov-Smirnov test (Cellquest Software) was used to compare FACS profiles.

**DISPLAY ITEMS: 5 figures**

**SUPPLEMENTARY DATA**

Supplementary data are provided: Supplementary methods, 5 supplementary figures and 3 Supplementary videos and 1 supplementary table.

**ACKNOWLEDGMENTS**

We thank A. Trautmann and B. Malissen for helpful discussions and critical reading of the manuscript. We thank J.F. Renaud and A. Lombet for continuous support and N. Kerlero de Rosbo for reading the manuscript. We thank B. Lucas for helpful discussions. We thank C. Rücker-Martin and V. Nicolas for advice and assistance on confocal microscopy, L. Dauphinot for expertise in PCR, D. Jaillard for excellent assistance with electron microscopy, J.P. Mauger and S. Wick for access to the animal facility. This work was supported by grants from *Association de la Recherche contre le Cancer* (to S.C-K and to T.C.), *Fondation de France* (to S.C-K), *Bonus Qualité Recherche de l'Université Paris-Sud* (to O.M. and S.C-K), *Centre National de la Recherche Scientifique*, *Conseil Régional Ile de France (Sesame)* and *Association Marie Lannelongue*. P.A was supported as a PhD candidate by a studentship from the *Ministère de l'Education nationale, de la Recherche et de la Technologie*. GLC and SP are supported by the Medical Research Council. GLC is a Royal Society-Wolfson Merit Award Holder.

**CONFLICT OF INTEREST**

The authors declare no conflict of interest

## REFERENCES

1. Mayer, ML and Armstrong, N, (2004) Structure and function of glutamate receptor ion channels. *Annu Rev Physiol* 66: 161-81.
2. Riedel, G, Platt, B and Micheau, J, (2003) Glutamate receptor function in learning and memory. *Behav Brain Res* 140: 1-47.
3. Nedergaard, M, Takano, T and Hansen, AJ, (2002) Beyond the role of glutamate as a neurotransmitter. *Nat Rev Neurosci* 3: 748-55.
4. Skerry, TM and Genever, PG, (2001) Glutamate signalling in non-neuronal tissues. *Trends Pharmacol Sci* 22: 174-81.
5. Pacheco, R, Gallart, T, Lluís, C and Franco, R, (2007) Role of glutamate on T-cell mediated immunity. *J Neuroimmunol* 185: 9-19.
6. Pacheco, R, Ciruela, F, Casado, V, Mallol, J, Gallart, T, Lluís, C et al., (2004) Group I metabotropic glutamate receptors mediate a dual role of glutamate in T cell activation. *J Biol Chem* 279: 33352-8.
7. Chiocchetti, A, Miglio, G, Mesturini, R, Varsaldi, F, Mocellin, M, Orilieri, E et al., (2006) Group I mGlu receptor stimulation inhibits activation-induced cell death of human T lymphocytes. *Br J Pharmacol* 148: 760-8.
8. Boldyrev, AA, Carpenter, DO and Johnson, P, (2005) Emerging evidence for a similar role of glutamate receptors in the nervous and immune systems. *J Neurochem* 95: 913-8.
9. Ganor, Y, Besser, M, Ben-Zakay, N, Unger, T and Levite, M, (2003) Human T cells express a functional ionotropic glutamate receptor GluR3, and glutamate by itself triggers integrin-mediated adhesion to laminin and fibronectin and chemotactic migration. *J Immunol* 170: 4362-72.
10. Lombardi, G, Miglio, G, Dianzani, C, Mesturini, R, Varsaldi, F, Chiocchetti, A et al., (2004) Glutamate modulation of human lymphocyte growth: in vitro studies. *Biochem Biophys Res Commun* 318: 496-502.
11. Lombardi, G, Dianzani, C, Miglio, G, Canonico, PL and Fantozzi, R, (2001) Characterization of ionotropic glutamate receptors in human lymphocytes. *Br J Pharmacol* 133: 936-44.
12. Miglio, G, Varsaldi, F and Lombardi, G, (2005) Human T lymphocytes express N-methyl-D-aspartate receptors functionally active in controlling T cell activation. *Biochem Biophys Res Commun* 338: 1875-83.

13. Lewis, RS, (2001) Calcium signaling mechanisms in T lymphocytes. *Annu Rev Immunol* 19: 497-521.
14. Vig, M, Peinelt, C, Beck, A, Koomoa, DL, Rabah, D, Koblan-Huberson, M et al., (2006) CRACM1 is a plasma membrane protein essential for store-operated Ca<sup>2+</sup> entry. *Science* 312: 1220-3.
15. Lioudyno, MI, Kozak, JA, Penna, A, Safrina, O, Zhang, SL, Sen, D et al., (2008) Orai1 and STIM1 move to the immunological synapse and are up-regulated during T cell activation. *Proc Natl Acad Sci U S A* 105: 2011-6.
16. Kotturi, MF, Hunt, SV and Jefferies, WA, (2006) Roles of CRAC and Cav-like channels in T cells: more than one gatekeeper? *Trends Pharmacol Sci* 27: 360-7.
17. Norcross, MA, (1984) A synaptic basis for T-lymphocyte activation. *Ann Immunol (Paris)* 135D: 113-34.
18. Huse, M, Lillemeier, BF, Kuhns, MS, Chen, DS and Davis, MM, (2006) T cells use two directionally distinct pathways for cytokine secretion. *Nat Immunol* 7: 247-55.
19. Brossard, C, Feuillet, V, Schmitt, A, Randriamampita, C, Romao, M, Raposo, G et al., (2005) Multifocal structure of the T cell - dendritic cell synapse. *Eur J Immunol* 35: 1741-53.
20. Dustin, ML and Colman, DR, (2002) Neural and immunological synaptic relations. *Science* 298: 785-9.
21. Steinman, L, (2004) Elaborate interactions between the immune and nervous systems. *Nat Immunol* 5: 575-81.
22. Pacheco, R, Oliva, H, Martinez-Navio, JM, Climent, N, Ciruela, F, Gatell, JM et al., (2006) Glutamate released by dendritic cells as a novel modulator of T cell activation. *J Immunol* 177: 6695-704.
23. Arundine, M and Tymianski, M, (2003) Molecular mechanisms of calcium-dependent neurodegeneration in excitotoxicity. *Cell Calcium* 34: 325-37.
24. Richie, LI, Ebert, PJ, Wu, LC, Krummel, MF, Owen, JJ and Davis, MM, (2002) Imaging synapse formation during thymocyte selection: inability of CD3zeta to form a stable central accumulation during negative selection. *Immunity* 16: 595-606.
25. Storto, M, de Grazia, U, Battaglia, G, Felli, MP, Maroder, M, Gulino, A et al., (2000) Expression of metabotropic glutamate receptors in murine thymocytes and thymic stromal cells. *J Neuroimmunol* 109: 112-20.
26. Collingridge, GL, Olsen, RW, Peters, J and Spedding, M, (2009) A nomenclature for ligand-gated ion channels. *Neuropharmacology* 56: 2-5.

27. Liblau, RS, Tisch, R, Shokat, K, Yang, X, Dumont, N, Goodnow, CC *et al.*, (1996) Intravenous injection of soluble antigen induces thymic and peripheral T-cells apoptosis. *Proc Natl Acad Sci U S A* 93: 3031-6.
28. Woronicz, JD, Calnan, B, Ngo, V and Winoto, A, (1994) Requirement for the orphan steroid receptor Nur77 in apoptosis of T-cell hybridomas. *Nature* 367: 277-81.
29. Cho, HJ, Edmondson, SG, Miller, AD, Sellars, M, Alexander, ST, Somersan, S *et al.*, (2003) Cutting edge: identification of the targets of clonal deletion in an unmanipulated thymus. *J Immunol* 170: 10-3.
30. Merckenschlager, M, Graf, D, Lovatt, M, Bommhardt, U, Zamoyska, R and Fisher, AG, (1997) How many thymocytes audition for selection? *J Exp Med* 186: 1149-58.
31. Winoto, A and Littman, DR, (2002) Nuclear hormone receptors in T lymphocytes. *Cell* 109 Suppl: S57-66.
32. Round, JL, Tomassian, T, Zhang, M, Patel, V, Schoenberger, SP and Miceli, MC, (2005) Dlg1 coordinates actin polymerization, synaptic T cell receptor and lipid raft aggregation, and effector function in T cells. *J Exp Med* 201: 419-30.
33. Kornau, HC, Schenker, LT, Kennedy, MB and Seeburg, PH, (1995) Domain interaction between NMDA receptor subunits and the postsynaptic density protein PSD-95. *Science* 269: 1737-40.
34. Kim, E and Sheng, M, (2004) PDZ domain proteins of synapses. *Nat Rev Neurosci* 5: 771-81.
35. Takamori, S, Rhee, JS, Rosenmund, C and Jahn, R, (2000) Identification of a vesicular glutamate transporter that defines a glutamatergic phenotype in neurons. *Nature* 407: 189-94.
36. Sudhof, TC, (2004) The synaptic vesicle cycle. *Annu Rev Neurosci* 27: 509-47.
37. Innocenti, B, Parpura, V and Haydon, PG, (2000) Imaging extracellular waves of glutamate during calcium signaling in cultured astrocytes. *J Neurosci* 20: 1800-8.
38. Bezzi, P, Domercq, M, Brambilla, L, Galli, R, Schols, D, De Clercq, E *et al.*, (2001) CXCR4-activated astrocyte glutamate release via TNF $\alpha$ : amplification by microglia triggers neurotoxicity. *Nat Neurosci* 4: 702-10.
39. Montes, M, McIlroy, D, Hosmalin, A and Trautmann, A, (1999) Calcium responses elicited in human T cells and dendritic cells by cell-cell interaction and soluble ligands. *Int Immunol* 11: 561-8.
40. Collingridge, GL, Isaac, JT and Wang, YT, (2004) Receptor trafficking and synaptic plasticity. *Nat Rev Neurosci* 5: 952-62.



41. Borg, C, Jalil, A, Laderach, D, Maruyama, K, Wakasugi, H, Charrier, S et al., (2004) NK cell activation by dendritic cells (DCs) requires the formation of a synapse leading to IL-12 polarization in DCs. *Blood* 104: 3267-75.
42. Trautmann, A, (2005) Chemokines as immunotransmitters? *Nat Immunol* 6: 427-8.
43. Augustine, GJ, Santamaria, F and Tanaka, K, (2003) Local calcium signaling in neurons. *Neuron* 40: 331-46.
44. Jun, JE, Wilson, LE, Vinuesa, CG, Lesage, S, Blery, M, Miosge, LA et al., (2003) Identifying the MAGUK protein Carma-1 as a central regulator of humoral immune responses and atopy by genome-wide mouse mutagenesis. *Immunity* 18: 751-62.
45. Palmer, E, (2003) Negative selection--clearing out the bad apples from the T-cell repertoire. *Nat Rev Immunol* 3: 383-91.
46. Potier, MC, Gibelin, N, Cauli, B, Le Bourdelles, B, Lambolez, B, Golfier, G et al., (2002) Development of microarrays to study gene expression in tissue and single cells: analysis of neural transmission. In *Microarrays for the Neurosciences: an essential guide*. (MIT Press) pp. 237-254.
47. Delon, J, Bercovici, N, Raposo, G, Liblau, R and Trautmann, A, (1998) Antigen-dependent and -independent Ca<sup>2+</sup> responses triggered in T cells by dendritic cells compared with B cells. *J Exp Med* 188: 1473-84.

## TITLES AND LEGENDS TO FIGURES

**Figure 1: T cells express a large array of i- and m-GluRs** (a) Oligoarray (Neurotrans<sup>TM</sup>) analysis of NMDAR mRNA expression on thymocytes compared to brain (upper panel), and validated by RT-PCR compared to brain (lower panel). Oligoarray data are displayed as a heat map. Data for all GluRs are shown in Supplementary Figure S1 using primers shown in Supplementary Table S1. (b) Immunofluorescence analysis of NMDAR subunit expression on thymocytes. For each indicated NMDAR subunit (NR1, NR2A, NR2B), a Nomarski image (left) and a confocal fluorescence image is shown in an equatorial plane (right). Images for other iGluRs are shown in Supplementary Figure S1c. Control staining consisting in IgG2b isotype control (for anti-NR1 antibody) or purified rabbit IgG (for anti-NR2A, NR2B, GluR2/3, KA2 antibodies) were negative using the same settings as the specific staining (Supplementary Figure S1c) (c) Flow cytometry analysis of NR1 expression in thymocytes. Relative fluorescence intensity is shown for CD4<sup>+</sup>, CD8<sup>+</sup> and DP subpopulations. Data are representative of 3 independent experiments. IgG2b control isotype is shown as control for NR1 staining.

**Figure 2: NMDAR modulates Ca<sup>2+</sup> signalling in thymocytes in contact with DCs, in the absence of exogenous glutamate**

(a) Representative time-lapse microscopy images (DIC/Fura-2 overlay) of thymocytes (upper set) and peripheral T cells (lower set) making contact with HA-pulsed DCs. The scale indicates Ca<sup>2+</sup> level, expressed as  $\Delta R/R$  values, ranging from 0 (blue) to 3 (red). In thymocytes, steep [Ca<sup>2+</sup>]<sub>i</sub> increases were recorded 44±3 s (n=101) after initial contact with the DC, and was, in most synapses, rapidly followed by the establishment of a stable contact (50±2 s, n=93) associated to a sustained high-level plateau lasting at least 10 minute (b) Representative Ca<sup>2+</sup> signal in Fura-2 loaded

thymocytes in contact with unpulsed DCs (left panel) or with HA-pulsed DCs (right panel) Arrows: contact. **(c)** Representative  $\text{Ca}^{2+}$  signal in Fura-2 loaded peripheral T cells in contact with HA-pulsed DCs. Arrow: contact. **(d)** Representative traces of the  $\text{Ca}^{2+}$  response in thymocytes in contact with HA-pulsed DCs in the presence (black curves) or absence (gray curves) of the NMDAR antagonists memantine (100  $\mu\text{M}$ ) (left panel) and MK801 (100  $\mu\text{M}$ ) (right panel). Arrows: contact.

**Figure 3: NMDAR triggers a sustained calcium signal, is transiently activated and is involved in caspase-3 activation and Nur77 induction, in thymocytes in contact with DCs**

**(a)** Inhibition of caspase-3 ( $t = 6$  h) expression in DP thymocytes co-cultured with unpulsed or HA-pulsed DCs with or without MK801 (100  $\mu\text{M}$ ) and memantine (100  $\mu\text{M}$ ). Data are means of six replicates for five independent cultures ( $*** P < 0.001$ ). The effect of memantine or MK801 on apoptosis was dose-dependent and was significant at 10  $\mu\text{M}$ , with the maximal effect observed at 100  $\mu\text{M}$ . A dose of 10  $\mu\text{M}$  MK801 resulted in  $11.4 \pm 1$  % inhibition of apoptosis ( $n=6$ ) and a transient  $\text{Ca}^{2+}$  signal in 50% thymocytes ( $n=10$ ) (data not shown). **(b)** Flow cytometry analysis of Nur77 expression in DP thymocytes, before and 4 hours after contact with antigen-loaded DCs, in the presence or absence of MK801 (100 $\mu\text{M}$ ). The graphs are representative of 3 experiments. **(c)** Quantification of Nur77 expressing DP thymocytes before and 4 hours after contact with antigen-loaded DCs, in the presence or absence of MK801 (100 $\mu\text{M}$ ). **(d)** Representative traces of the  $\text{Ca}^{2+}$  response in thymocytes in contact with HA-pulsed DCs. Thymocytes were preincubated with MK801 (100 $\mu\text{M}$ ), NMDA (300  $\mu\text{M}$ ) and D-serine (20  $\mu\text{M}$ ) to block any NMDARs that would be present at the membrane before synapse formation. Thymocytes were then washed and added to HA-pulsed DCs in the absence or presence of the NMDAR antagonists MK801 (100  $\mu\text{M}$ ).

(e) Representative traces of the  $\text{Ca}^{2+}$  response in thymocytes in contact with HA-pulsed DCs MK801 (100  $\mu\text{M}$ ) was applied after the beginning of  $\text{Ca}^{2+}$  response ( $t=208$  s).

**Figure 4: TCR triggering is sufficient to induce NMDAR relocation at the thymocyte-DC contact zone, while MDAR can be activated only in a synaptic context.** (a) Double labeling of PSD-95 (red) and NR1 (green) on isolated thymocytes, thymocytes in contact with anti-CD3/CD28-coated beads and thymocytes in contact with a DC. Merged pictures are shown in each case (yellow), Scale bars, 10  $\mu\text{m}$ . Profiles of distribution of fluorescence intensities and colocalization analysis of PSD-95 and NR1 are shown in Supplementary Figure S4. Controls consisted in mouse IgG2b isotype control for NR1 and purified rabbit IgG for PSD-95 (not shown). (b) Representative trace of  $\text{Ca}^{2+}$  response in thymocytes in contact with anti-CD3/CD28 coated beads. Arrow: contact. (c) Histogram of the mean  $\text{Ca}^{2+}$  amplitudes from 6 to 11 representative traces at the initial peak and at the plateau phase (600 s after the initial peak), in the absence or presence of glutamate (300  $\mu\text{M}$ ) and NMDA (100  $\mu\text{M}$ ).

**Figure 5: DCs may be the physiological source of glutamate in T cell-DC synapses** (a) Confocal immunofluorescence image of glutamate labeling in a DC in contact with three thymocytes (right). Corresponding Nomarski image (left), with an inset indicating the cell contours. Scale bar, 10  $\mu\text{m}$ . (b) Immunofluorescence analysis of VGLUT1, VGLUT2 and VGLUT3 in DCs (bottom row), with the corresponding Nomarski images (top row). Scale bar, 10  $\mu\text{m}$ . Typical punctate fluorescent staining of VGLUT2 and VGLUT3, similar to that observed in neurons, was observed in DCs (Supplementary Figure S5b). (c) Morphological electron micrograph of T cell-DC conjugates showing a group of vesicle structures at the cell-cell interface. Original image (left, scale bar, 2  $\mu\text{m}$ ). Magnification of the synapse (middle, scale bar, 100 nm) and of the vesicles (right, scale

bar, 100 nm). Arrows: individual vesicles in the DC. **(d)** Immunogold staining of VGLUT2 in the T cell-DC contact zone. Top: low magnification with vesicles in the DC indicated by arrows. Bottom: higher magnification. Scale bar, 100 nm. **(e)** Immunogold colocalization of VGLUT2 (5 nm) and synaptotagmin I (10 nm) on the same vesicular structures (arrows). Top: individual vesicles indicated by arrows (scale bar, 2  $\mu$ m). Bottom: magnifications (scale bars, 100 nm). Control staining is shown in Supplementary Figure S5d **(f)** Typical traces of glutamate release (upper panels) from DCs stimulated with ionomycin (1  $\mu$ M), monitored in continuous culture, by recording NADH fluorescence emission. Horizontal scale: time in seconds. Vertical scale: arbitrary units. The amounts of glutamate released represented 40 % of the fluorescence increase induced by 10  $\mu$ M glutamate. Lower panels:  $\text{Ca}^{2+}$  signals induced by ionomycin in the presence or absence of extracellular  $\text{Ca}^{2+}$  in Fura-2-loaded DCs. **(g)** Typical traces of glutamate release (upper panel) from DCs stimulated with SDF-1 $\alpha$  (100 nM), monitored as in **(f)**. Vertical scale: arbitrary units. Lower panel:  $\text{Ca}^{2+}$  signal induced by SDF-1 $\alpha$  in Fura-2-loaded DCs, in the presence of extracellular  $\text{Ca}^{2+}$ .

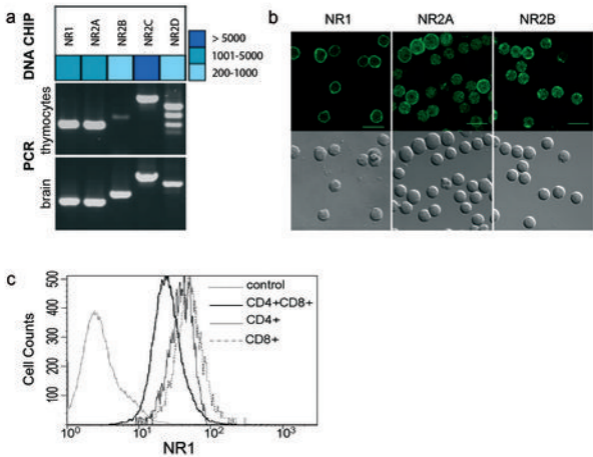


Figure 1 (Affaticati *et al.*)

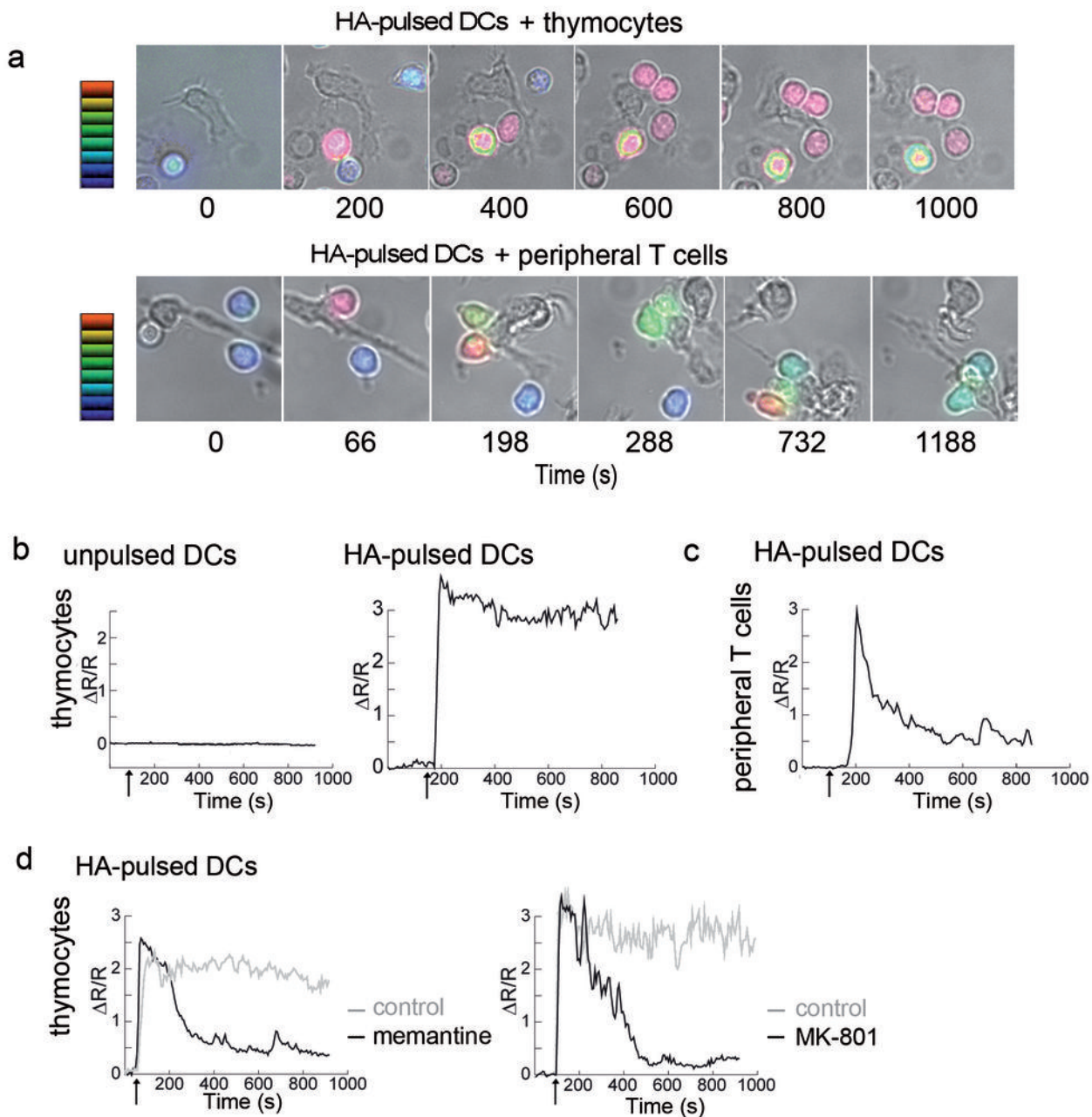
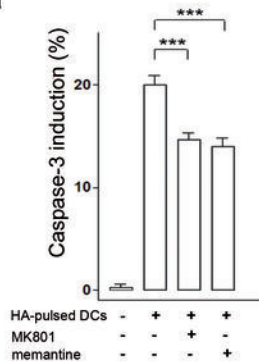
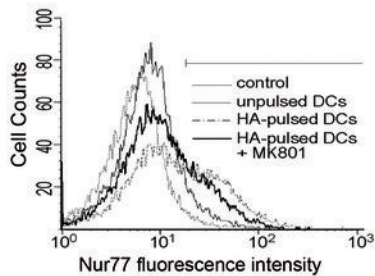
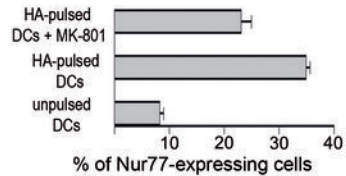
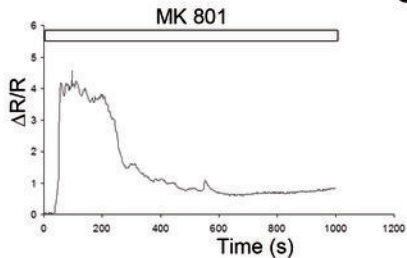
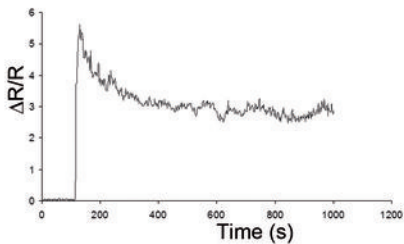
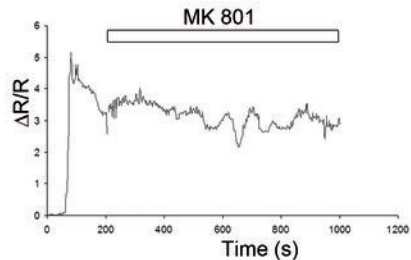


Figure 2 (Affaticati *et al.*)

**a****b****c****d****e**Figure-3 (Affaticati *et al.*)



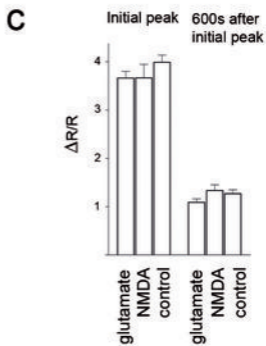
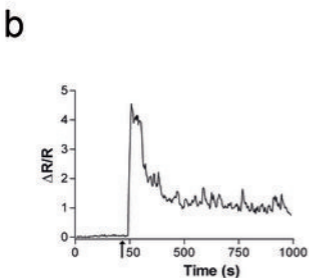
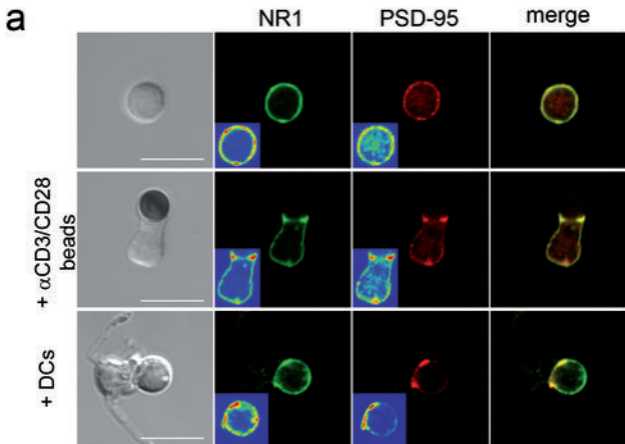


Figure 4 (Affaticati *et al.*)

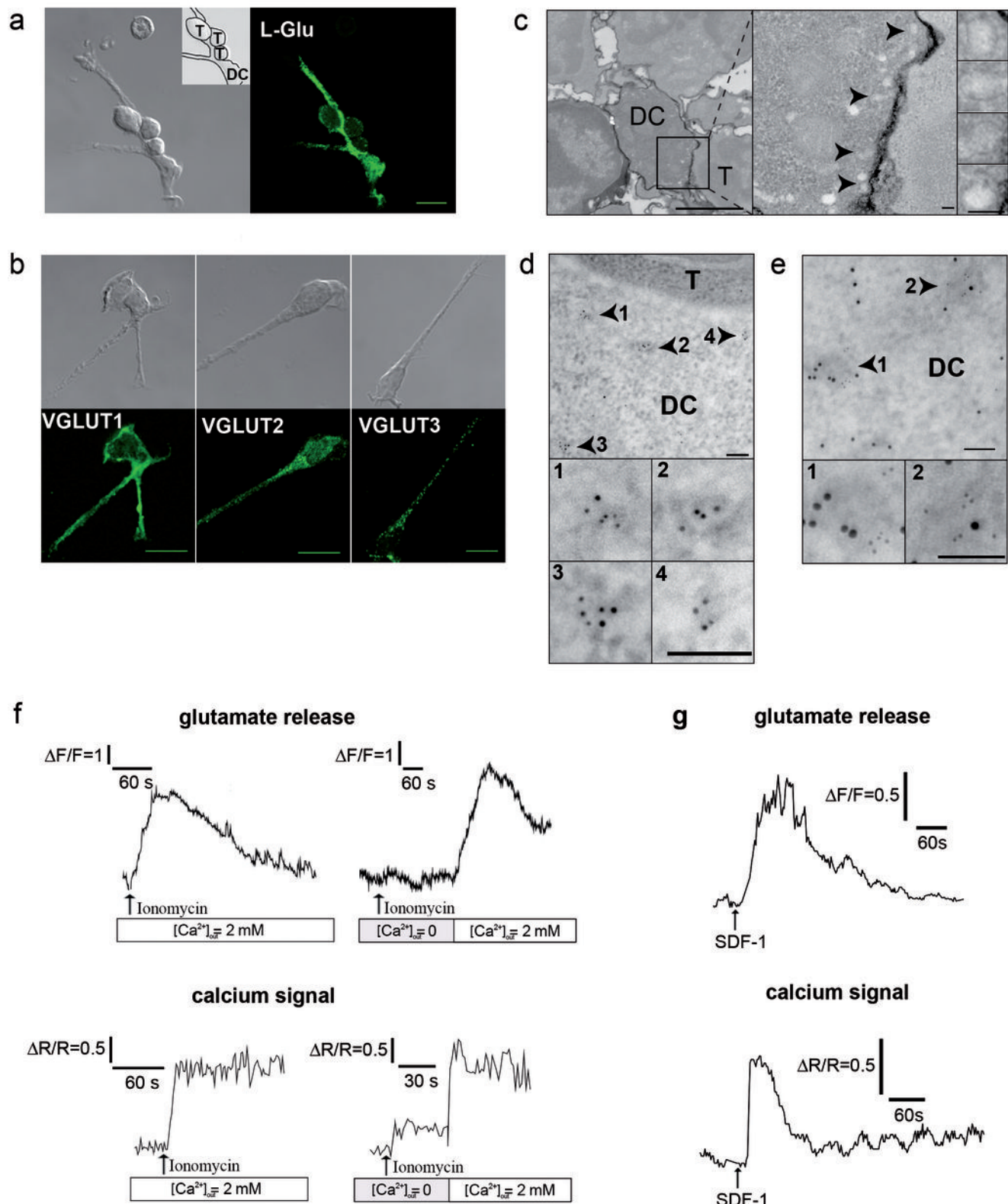


Figure 5 (Affaticati et al.)